NASA Contractor Report 187459

ICASE Report No. 90-75

ICASE

"OPTIMUM" UPWIND ADVECTION ON A TRIANGULAR MESH

P. L. Roe

NASA

National Aeronautics and
Space Administration

Langley Research Center
Hampton, Virginia 23665-5225

"OPTIMUM" UPWIND ADVECTION ON
A TRIANGULAR MESH

P. L. Roe[1]
Department of Aerospace Engineering
University of Michigan

ABSTRACT

For advection schemes based on fluctuation splitting, a design criterion of optimising the time step leads to linear schemes that coincide with those designed for least truncation error. A further stage of optimising the time step using a non-linear positivity criterion, leads to considerable further gains in resolution.

1. Introduction

This note is a contribution to the development of high resolution advection schemes for use on (possibly) unstructured triangular meshes. The search is for a scheme that is positive (admitting no new extrema) and as accurate as possible. Such schemes have an inherently nonlinear dependence on the data, and revert near discontinuities to an essentially first-order behavior. It is of interest to know what is the optimum positive first-order scheme, so that performance near discontinuities is not excessively degraded.

The schemes considered in this paper belong to a class introduced in [1], and explored more thoroughly in [2]. These papers, and also [3], should be consulted for more background.

2. Previous Work

Consider a triangular grid of which Figure 1 shows a generic element. On such a grid, we wish to solve the two-dimensional advection equation

$$u_t + \underline{a} \cdot \nabla u = 0, \tag{1}$$

where $\underline{a}$ is a constant vector $(a, b)^T$.

For each triangular element T define the "fluctuation"

$$\phi^T = \int\int_T u_t dx dy.$$

By Equation (1) and Gauss' theorem

$$\phi^T = \oint u \, \underline{a} \cdot d\underline{n}.$$

If u is assumed to vary linearly over the triangle

$$\phi^T = -\sum k_i u_i, \tag{2}$$

where

$$k_i = \frac{1}{2}\underline{a} \cdot \underline{n}_i, \tag{3}$$

and n_i is the inward (scaled) normal to the side opposite v_i. Note that

$$\sum k_i = 0$$

so that either one or two k_i are positive. Geometrically, this corresponds to the vector **a** crossing either one or two sides in the inward direction.

In [1,2] it is shown that part of a positive update process is to add, in the case of one inflow side (which we call a type I triangle, Figure 2a) a quantity $\Delta t \phi_T$ to the single downstream vertex. If this is v_i, then

$$S_i u_i^{u+1} = S_i u_i^n + \Delta t \phi^T + (\cdot) \tag{4}$$

where $(\cdot)$ signifies the contributions, if any, coming from other triangles neighboring v_i, and S_i is one-third the area of those triangles having v_i as a vertex.

In the difficult case where there are two inflow sides, say those opposite vertices i and j (a type II triangle) the proposed scheme is

$$S_i u_i^{u+1} = S_i u_i^u + \alpha_i \Delta t \phi^T + (\cdot) \left.\right\}$$
$$S_i u_j^{u+1} = S_j u_j^u + \alpha_j \Delta t \phi^T + (\cdot) \left.\right\} \tag{5}$$

where, from a conservation argument,

$$\alpha_i + \alpha_j = 1.$$

It was proved in [1] (see also [2]) that no choice of α_i, α_j depending only on the geometry of the triangle and its relation to the flow vector can give a positive scheme. The nonlinear choice, which we call S1,

$$\alpha_i = k_i(u_i - u_k)/\phi^T \left.\right\}$$
$$\alpha_j = k_j(u_j - u_k)/\phi^T \left.\right\} \tag{6}$$

was advocated in [1] on the grounds that it permitted a larger timestep than any other choice (within a certain class). This scheme was found to be superior to regular finite-volume upwinding in [2, 3] and we will point out in the next section that it bears an interesting relationship to a recently published scheme of Sidilkover [4].

3. A Property of the Scheme S1

Substituting (6) into (5) gives the simple update method

$$S_i u_i^{u+1} = S_i u_i^n - k_i \Delta t(u_i^n - u_k^n) + (\cdot) \left.\right\}$$
$$S_j u_j^{u+1} = S_j u_j^n - k_j \Delta t(u_j^n - u_k^n) + (\cdot) \left.\right\} \tag{7}$$

Let us see what (7) reduces to on a square mesh of side h. We assume that a, b are both positive with $a \geq b$, and that the squares are divided into triangles along the diagonal with positive slope, as in Figure 3a. Freedom to cut the squares along either diagonal greatly enhances the performance of the schemes (R. Struijs, H. Deconinck, private communication, von Karman Institute).

Each point then receives contributions from three triangles, A, B, C, in which the fluctuations are

$$\phi^A = -\frac{1}{2}[(a - b)(u_0 - u_3)h + b(u_1 - u_3)h]$$

$$\phi^B = -\frac{1}{2}[a(u_0 - u_3)h + \underline{b(u_3 - u_4)h}]$$

$$\phi^C = -\frac{1}{2}[(a - b)(u_5 - u_4)h + \underline{b(u_0 - u_4)h}].$$

In each case, the fluctuations have been split as they would be by S1, and those terms contributing to the update of u_0 have been underlined. Summing those terms, we find

$$u_0^{n+1} = u_0^n - \frac{\Delta t}{h}[a(u_0 - u_3) + b(u_3 - u_4)]. \tag{8}$$

2

This is the scheme recently shown by Sidilkover [4] to have the least truncation error among the linear monotone schemes for solving (1). It comes in eight different flavors depending on the flow direction (Figure 4). (It may be remarked that whether the scheme is linear or nonlinear depends on the viewpoint. Clearly (7) has constant coefficients, but they change as the vector $\underline{a}$ moves into different octants. Written in the form (5), (6) the expressions that accomplish this switching give the appearance of nonlinearity.) Sidilkover [4] calls (7) the N-scheme because it has a narrow stencil and, not by coincidence, yields narrow discontinuities.

Now consider the squares divided along the other family of diagonals as in Figure 3b. The fluctuations in the triangles adjoining 0 are

$$\phi^A = -\underline{a(u_0 - u_3)} - b(u_2 - u_3)$$

$$\phi^B = -\underline{a(u_0 - u_3)} - \underline{b(u_0 - u_5)}$$

$$\phi^C = -a(u_6 - u_5) - \underline{b(u_0 - u_5)}$$

and scheme S1 will credit the underlined terms to 0. The update formula is

$$u_0^{u+1} = u_0^u - \frac{\Delta t}{h}[a(u_0 - u_3) + b(u_0 - u_5)] \tag{9}$$

which is just regular upwinding. For steady flows, the dissipation coefficient of (9) is

$$\frac{h}{2}|\sin\theta\cos\theta|\{|\sin\theta| + |\cos\theta|\}$$

whereas the dissipation coefficient of (8) is

$$\frac{h}{2}|\sin\theta\cos\theta|\,|\cos\theta - \sin\theta|$$

which is, on average, about four times smaller. There seems no reason why one should not take advantage of this by choosing the triangulation appropriate to the problem. In the non-linear case, of course, the choice might change with time.

4. Type II Triangles Revisited

The observation is made in [1, 2] that within each triangle T the advection velocity $\underline{a}$ can be replaced by

$$\underline{a}^T = \underline{a} + \lambda \underline{a}_p^T \tag{10}$$

where $\underline{a}_p^T$ is orthogonal to ∇u^T and λ is an arbitrary parameter. This is tantamount to saying that only the component of $\underline{a}$ normal to the level lines of the solution is relevant (Figure 5). In any analysis relating to events within the triangle T, $\underline{a}$ can be replaced by $\underline{a}^T$. There is an intuitive attraction to making $\underline{a}^T$ as small as possible, that is, taking it in the direction ∇u^T. Then we have

$$\underline{a}_{\min}^T = \left(\frac{\underline{a} \cdot \nabla u^T}{\nabla u^T \cdot \nabla u^T}\right)\nabla u^T = \frac{\phi^T \nabla u^T}{\nabla u^T \cdot \nabla u^T}. \tag{11}$$

3

A practical disadvantage to (9) is that in any region where the solution is almost uniform, the numerator and denominator are both very small, and numerical expressions based on (9) become ill-formed. This leads to slow, or halted, convergence. In [2], the expedient was taken of abandoning (9) gradually in favor of $\underline{a}$ in regions where $|\nabla_u^T|$ is small. Below, we will argue that (9) is anyway not optimal; the improved version leads also to better formed expressions.

We commence the analysis by noting that if (10) is substituted into (3) we have

$$k_i \;=\; \underline{a}^T \cdot \underline{n}_i$$

$$\;=\; \underline{a} \cdot \underline{n}_i + \lambda \underline{a}_p^T \cdot \underline{n}_i.$$

In the second inner product, $\underline{a}_p^T$ is orthogonal to ∇u and $\underline{n}_i$ is orthogonal to $\underline{s}_i$ where $\underline{s}_i$ is the vector along the side opposite v_i). Therefore

$$k_i = \underline{a} \cdot \underline{n}_i + \lambda u \cdot \underline{s}_i \tag{12}$$

so that

$$
\left.
\begin{aligned}
k_1 &= k_1^* + \lambda(u_3 - u_2) \\[4pt]
k_2 &= k_2^* + \lambda(u_1 - u_3) \\[4pt]
k_3 &= k_3^* + \lambda(u_2 - u_1)
\end{aligned}
\right\}
\tag{13}
$$

Here, k_1^*, k_2^*, k_3^* are the original coefficients computed from (3), and equations (13) define a one-parameter family of equally valid alternatives.

We pose the problem of choosing the k's so as to maximize the allowable time-step of the scheme. This is clearly a desirable objective in itself but heuristically it seems to lead to gains in accuracy also. (In one dimension, this criterion would lead us to classical upwinding and in Section 3, we saw that it led to the optimum linear schemes in two dimensions.) From (7), the scheme is positive for Type II triangles, if

$$\Delta t \leq \frac{1}{n} \min \left[\frac{S_i}{k_i}, \frac{S_j}{k_j} \right]$$

where i, j are the downwind vertices, and where n is the maximum number of triangles meeting at a point. Therefore, the relevant criterion is that

$$K = \max \left[\frac{k_i}{S_i}, \frac{k_j}{S_j} \right] \tag{14}$$

should be positive but as small as possible.

Consider a diagram of which the axes are $(k_i/S_i), (k_j/S_j)$. As λ varies, a straight line locus will be swept out whose slope is

$$\Lambda = -\frac{S_i(u_i - u_k)}{S_j(u_j - u_k)}.$$

4

Figure 6 shows such loci for given k_i^*, k_j^* (i.e., given geometry) for a range of Λ (i.e., a range of data). For each locus, a star marks the point that minimizes K.

If the star falls on the vertical axis, the decision is to update only the point j; on the horizontal axis we update only the point i. On the 45° line we have

$$\frac{k_i}{S_i} = \frac{k_j}{S_j}$$

so that, from (7)

$$\frac{\delta u_i^T}{\delta u_j^T} = \frac{u_i - u_k}{u_j - u_k} \tag{15}$$

(where δu_i^T means the change at vertex$_i$ due to this triangle). This corresponds to keeping the direction of ∇u constant during the update process. Figure 6 demonstrates that this is the best policy whenever Λ is negative, i.e., $(u_i - u_k), (u_j - u_k)$ have the same sign. An equivalent criterion is that the level line of the solution through v_k does not pass through the triangle. If the level line does pass through the triangle, we will only update one vertex. Which vertex is chosen will depend whether the locus in Figure 6 passes above or below the origin, and it is easy to demonstrate that this depends on the sign of ϕ^T.

The update algorithm is in fact, in pseudo-Fortran

```
If (only k_i.gt.0)
   update v_i
   goto end
endif
If (only k_k.lt.0) then
   If ((u_i - u_k)(u_j - u_k).gt.0) then
     update u_i, u_j
   else if ((u_i - u_k)φ^T.lt.0) then
     update u_i
   else
     update u_j
   endif
endif.
```

There are actually twelve different paths through this logic, although only six different outcomes. It can be verified that the updates at the vertices depend C° continuously on all aspects of the data. The only part of the algorithm that is badly formed arises if both u_i, u_j are to be updated, in accordance with (15). The explicit formulae are then

$$\delta u_i^T = \frac{u_i - u_k}{S_i(u_i - u_k) + S_j(u_j - u_k)} \phi^T \Delta t \tag{16a}$$

$$\delta u_j^T = \frac{u_j - u_k}{S_i(u_i - u_k) + S_j(u_j - u_k)} \phi_T \Delta t \tag{16b}$$

5

and it is possible for the denominator to be small. However, we only reach this situation if $(u_i - u_k)(u_j - u_k)$ are of the same sign, so they must be small individually, and ϕ_T must also be small. Thus, that triangle is in equilibrium, and can be ignored. In practice, we may test to see if ϕ_T is less than some moderate multiple of machine zero.

We call this the NN scheme, signifying non-linear and narrow.

5. Results and Discussion

The schemes will be demonstrated on two test problems shown in Figure 7.

The first problem is to solve the equation

$$u_t + u_x + \frac{1}{2}u_y = 0$$

on the unit square with $u = 1$ specified on the left edge and $u = 0$ on the bottom edge. This is the direction for which the N, and NN, schemes will show least advantage. The second problem is to solve the equation

$$u_t + x\,u_y - yu_x = 0$$

on the domain $n\epsilon[-1,1]$, $y\epsilon[0,1]$. The characteristic lines here are circles centered on the origin.

On all inflow boundaries we specify $u = 0$, except that on $y = 0$, we set $u = 1$ for $x\epsilon[-\frac{2}{3}, -\frac{1}{3}]$. The steady solution of this problem is therefore

$$u \;=\; 1 \quad \text{if} \quad 1 \le 9(x^2 + y^2) \le 4$$

$$=\; 0 \;\;\text{otherwise.}$$

In particular, when we plot $u(x,0)$ we expect, or at least hope, to see the input data for $x < 0$ mirrored in the solution for $x > 0$. An interesting feature of examining the solution in that way is that the dissipation error has been effectively integrated over all flow directions.

Figure 8(a) contains results from the regular upwind scheme for Problem 1 on a mesh of 31×31 nodes. The solution is very diffused, but would be even worse at a direction of $45°$. Figure 8(b) is obtained from the S1 scheme, but the mesh is triangulated in no preferential direction (Figure 7(c)). The results are very slightly improved, although this cannot be determined from the plots.

A very noticeable improvement comes from deploying the S1 scheme on a mesh triangulated along the upgoing diagonals. The results are shown in Figure 8(c), and precisely the same results are obtained using the N scheme on a square mesh. The discontinuity is resolved over about half the number of mesh points. It is worth remarking that this reduces by a factor of about 16 the computing cost of obtaining a solution with given resolution, because half as many points are needed in each direction, half as much time is needed to expel transients, and twice the timestep can be taken.

In Figure 8(d) we see results from the nonlinear scheme NN. Even on the isotropic mesh, these are the best so far, but by choosing the correct triangulation, the further improvement of Figure 8(e) is reached. Since this improves the resolution by a factor of 4, the cost at

given resolution is reduced by about a factor of 64. Recall that the results from the optimum scheme are actually worse for this flow angle. It is gratifying that the convergence history is scarcely affected by any of these improvements. The residual stays almost constant for about 80 timesteps, by which time the initial guess $u \equiv 0$ has been purged by the wave crossing the domain; after a further 70 to 80 timesteps, the solution is effectively converged. All tests were made at a Courant number of 0.5, but in fact the optimum scheme could have been run faster.

In Figure 9(a), the results are shown of the rotating advection problem on a mesh of 61 cells by 31 cells. Only the results for an optimized mesh are shown; the squares are cut by their upgoing diagonals for $x < 0$, by their downgoing diagonals for $x > 0$. The square pulse is preserved quite remarkably for a first-order scheme. Indeed, one may suspect that the step function is some kind of eigenmode for the scheme, and that all data will be squared-off, as happens for certain one-dimensional limiter schemes. To check this point, a narrow Gaussian pulse was substituted as data and was again preserved rather well (Figure 9(b)).

To make some kind of comparison with regular upwinding, the calculation in Figure 9(c) was performed. To give the regular scheme a chance, four times as many mesh points were used in each direction, i.e., 241×121. Even so, a very inferior result is achieved. In comparison with the straight advection test, the optimum schemes show in a better light and the regular scheme in a worse light. Their resolving powers differ here by a factor of about 10, and the cost of achieving given resolution changes by a factor of about one thousand.

6. Concluding Remarks

The schemes derived here have features with no close one-dimensional counterparts. They actively select the stencil to be used, and the connectivity of the mesh, and depend non-linearly on the data, all in the search for an optimal first-order scheme. They are of course to be viewed as the first phase in a quest for higher-order schemes that may exploit the same features. Nevertheless, their practical use in simulations of mixing and turbulent flows may not be out of the question. The resolution that they achieve compares favorably with that of formally higher-order schemes, and because all their operations are highly localized, the schemes are very suitable for parallel implementation.

7

References

[1] P. L. Roe, "Linear advection schemes on triangular meshes," CoA Report No. 8720, Cranfield Institute of Technology, November 1987.

[2] H. Deconinck, R. Struijs, P. L. Roe, "Fluctuation splitting for multidimensional convection problems: An alternative to finite volume and finite element methods," Von Karman Institute Lecture Series 1990-03 "Computational Fluid Dynamics."

[3] P. L. Roe, H. Deconinck, R. Struijs, "Recent progress in multidimensional upwinding," Proceedings 12th International Conference on Numerical Methods in Fluid Dynamics, Oxford, 1990, Springer, to appear.

[4] D. Sidilkover, "Numerical solution to steady-state problems with discontinuities", Ph.D. thesis, The Weizmann Institute, Rehovot, Israel, 1990
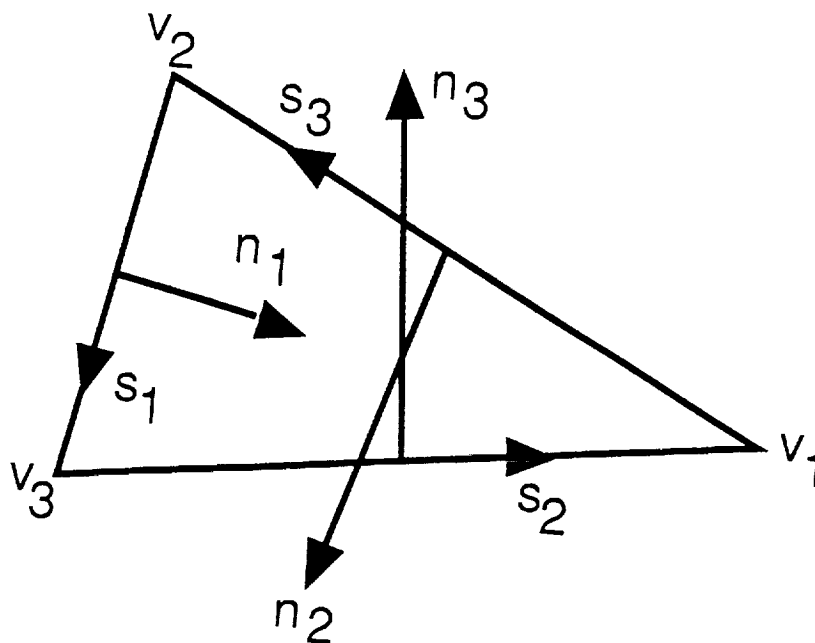
Figure 1. Notation to describe a typical triangle.

(a) Type I triangle   (b) Type II triangle
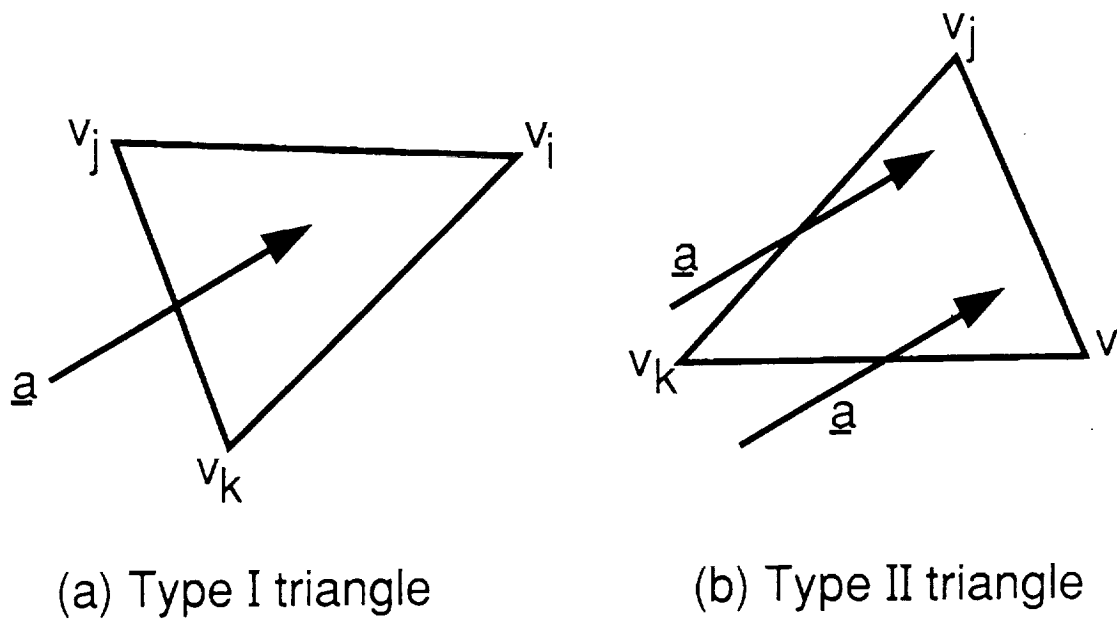
Figure 2. Triangles with one or two inflow sides.
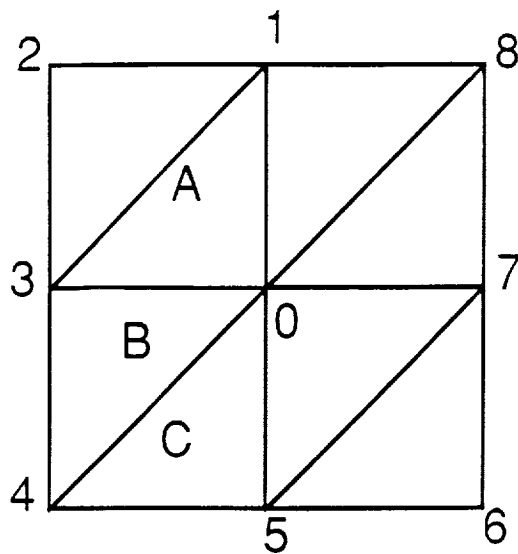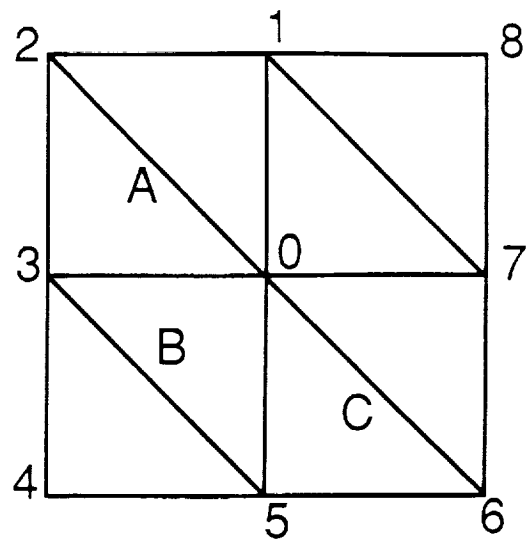
Figure 3. Square cells divided either correctly (a) or incorrectly (b) for flow with a, b both positive.
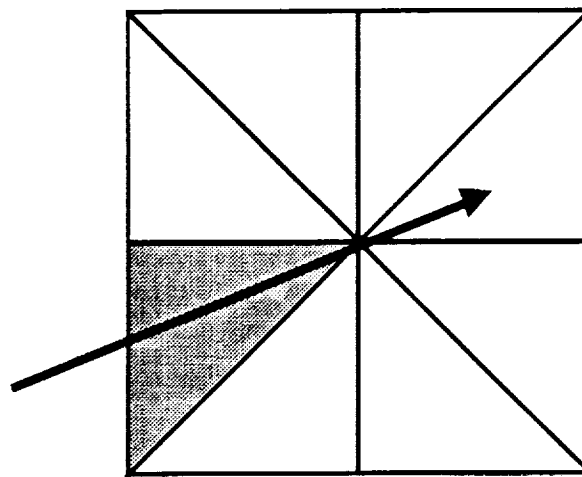
Figure 4. In the N-scheme, point O is updated using whichever triangle contains the incoming characteristic.
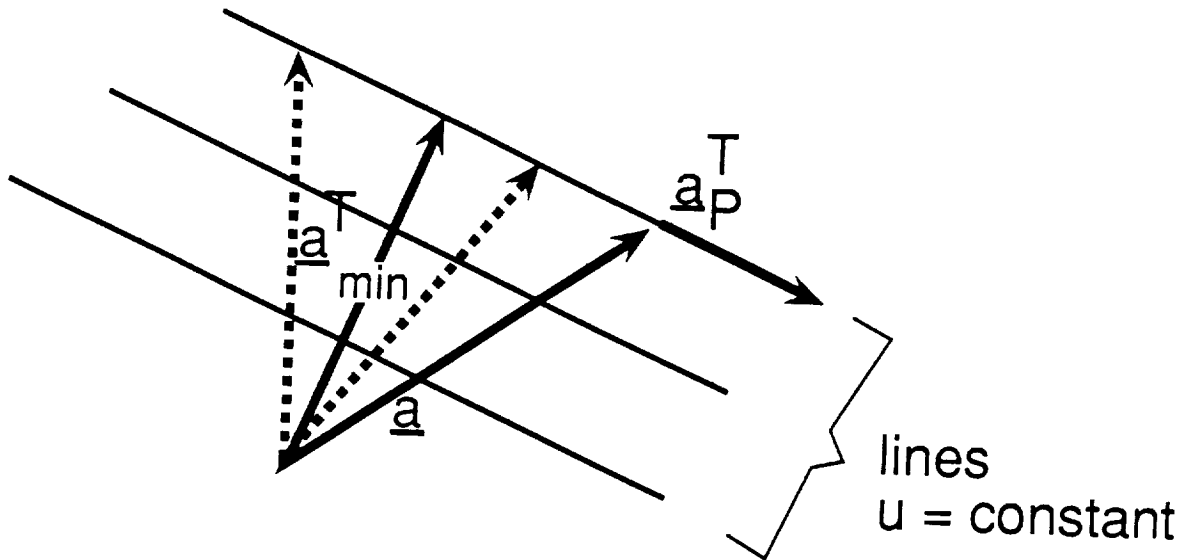
Figure 5. The set of equivalent advection vectors.
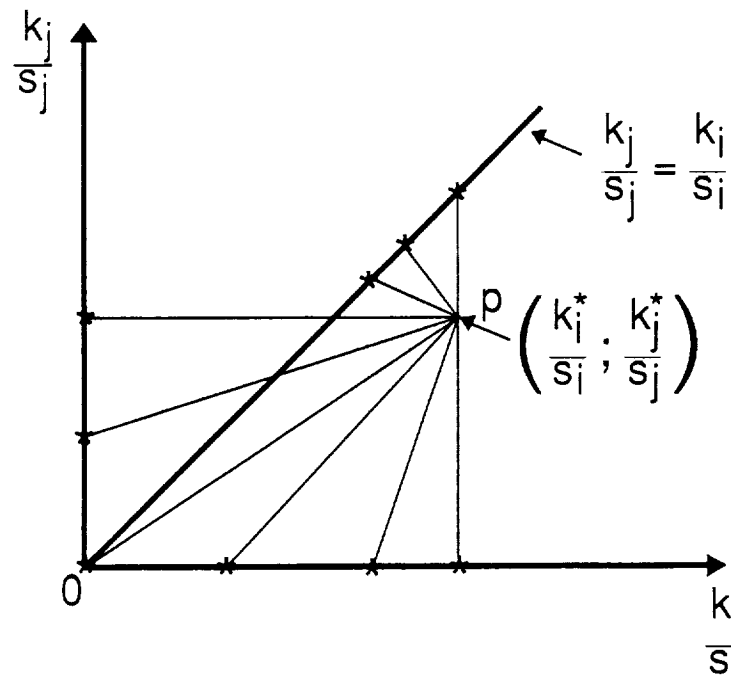
Figure 6. The minimax problem that determines the largest allowable timestep.

11
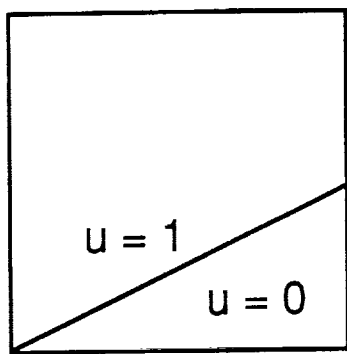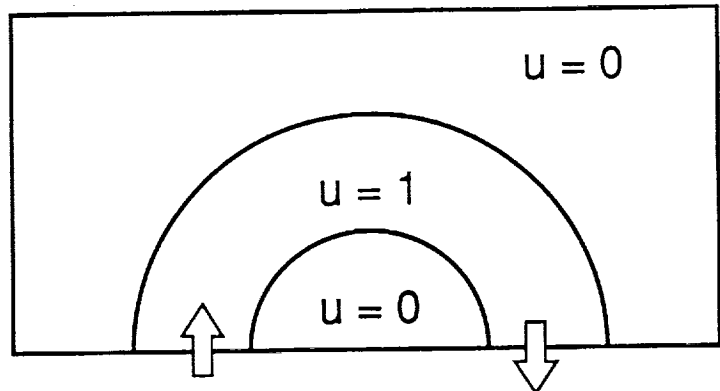
(a) Problem 1

(b) Problem 2
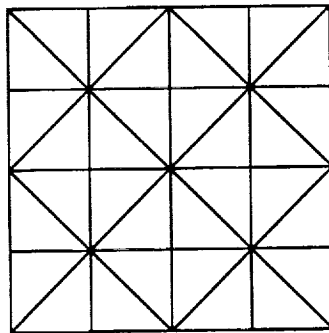
(c) Section of 'isotropic' mesh

Figure 7. The Test Problems.
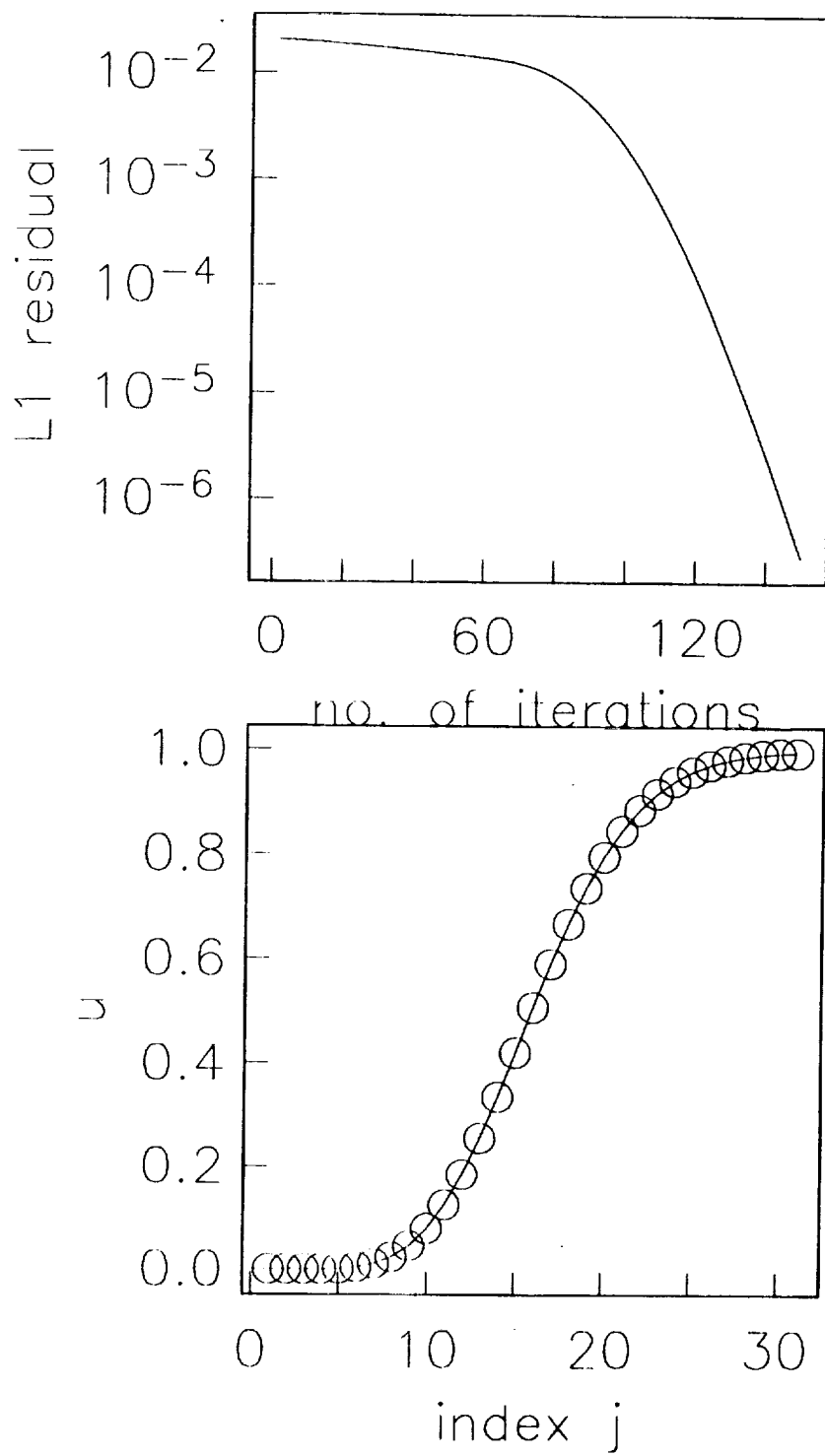
Figure 8(a) Problem 1 – regular upwinding
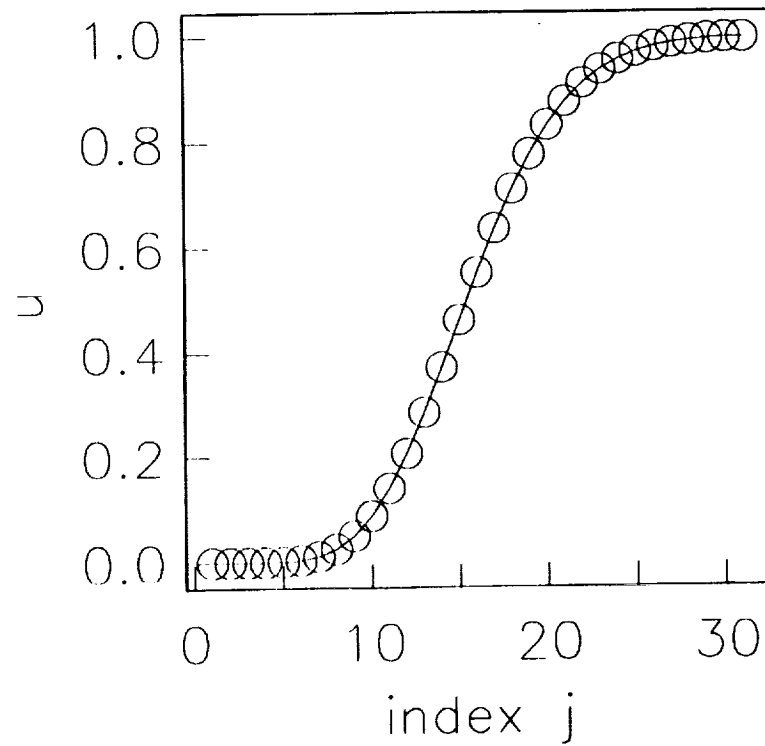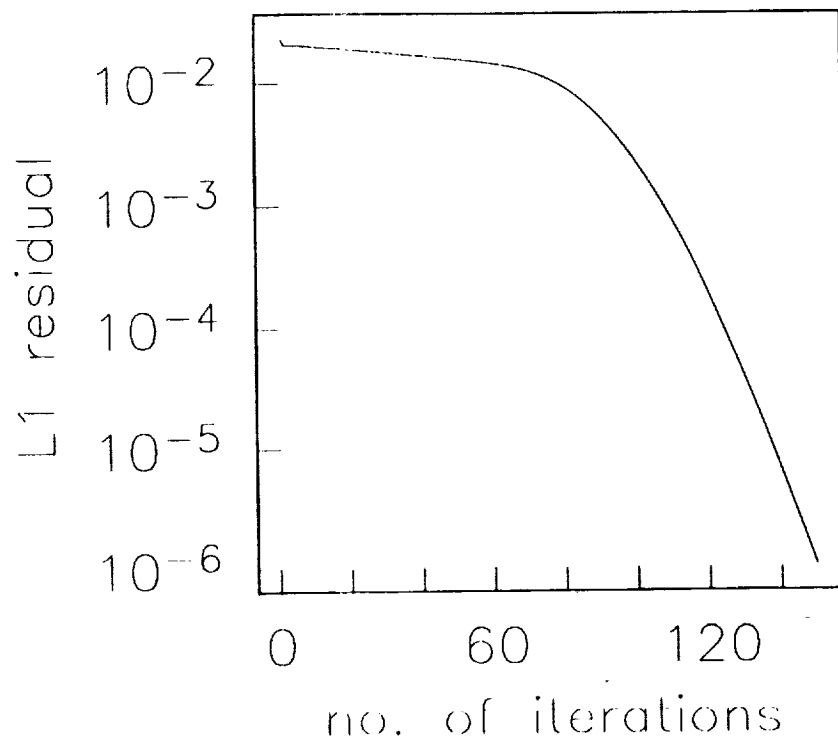
Figure 8(b) Problem 1, Scheme S1, isotropic mesh.

14
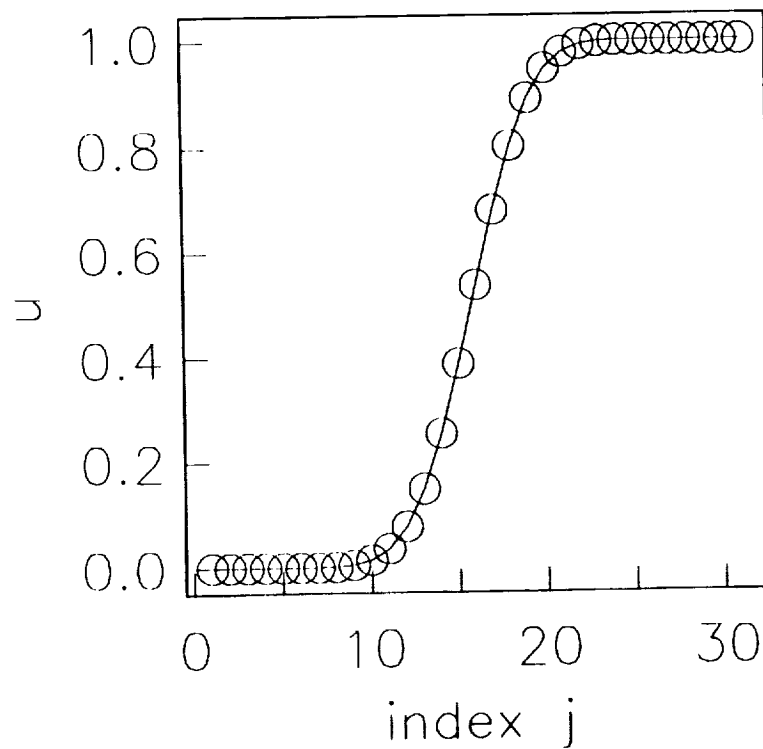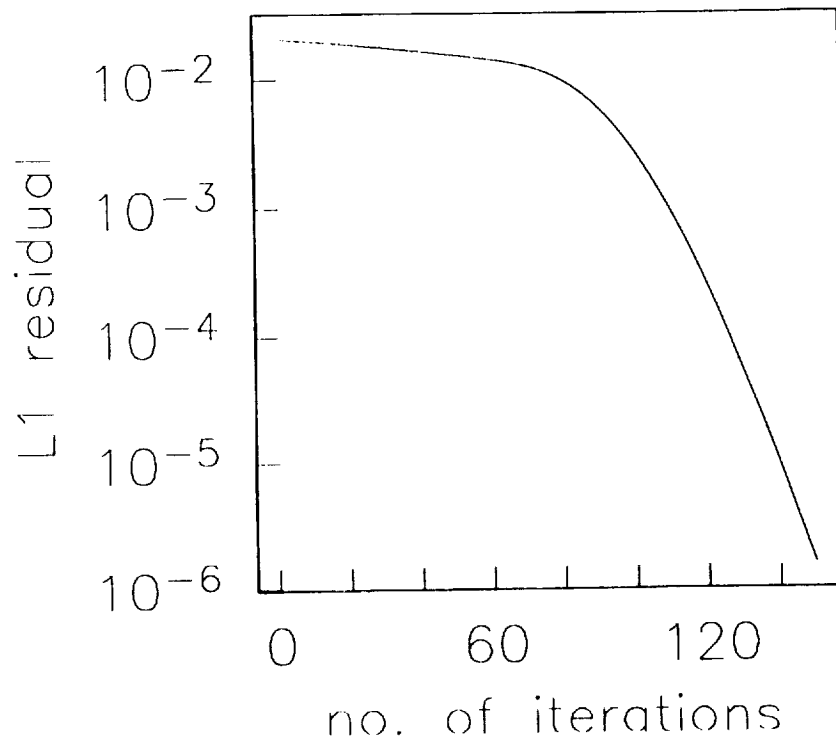
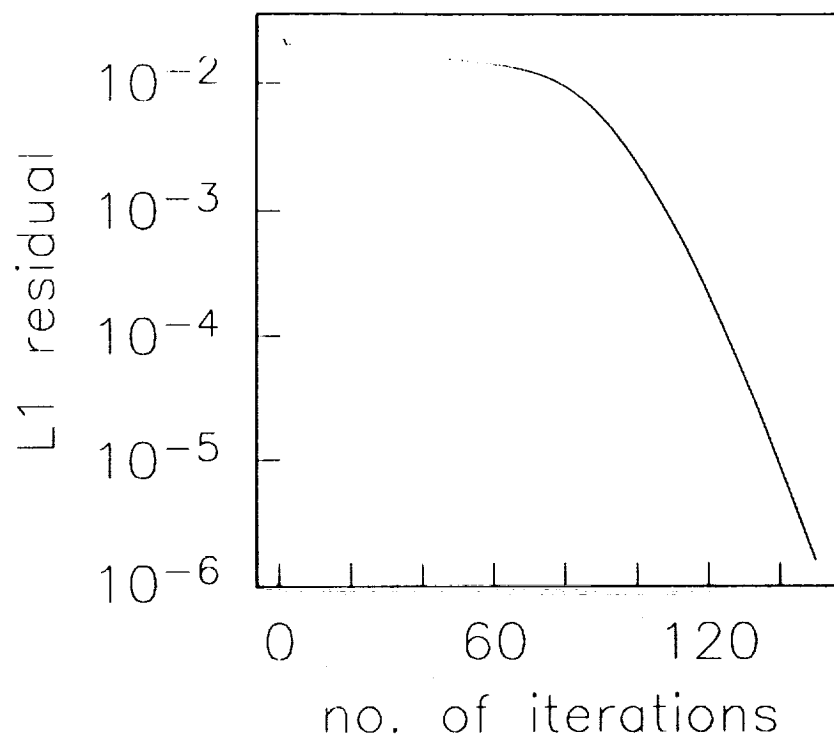Figure8(c) Problem 1, Scheme N or S1, correctly triangulated grid.
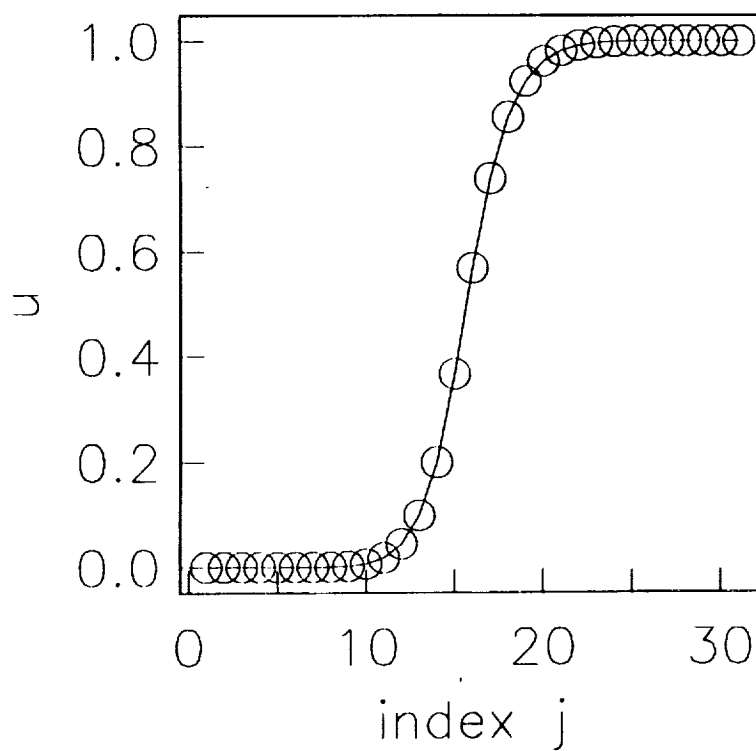
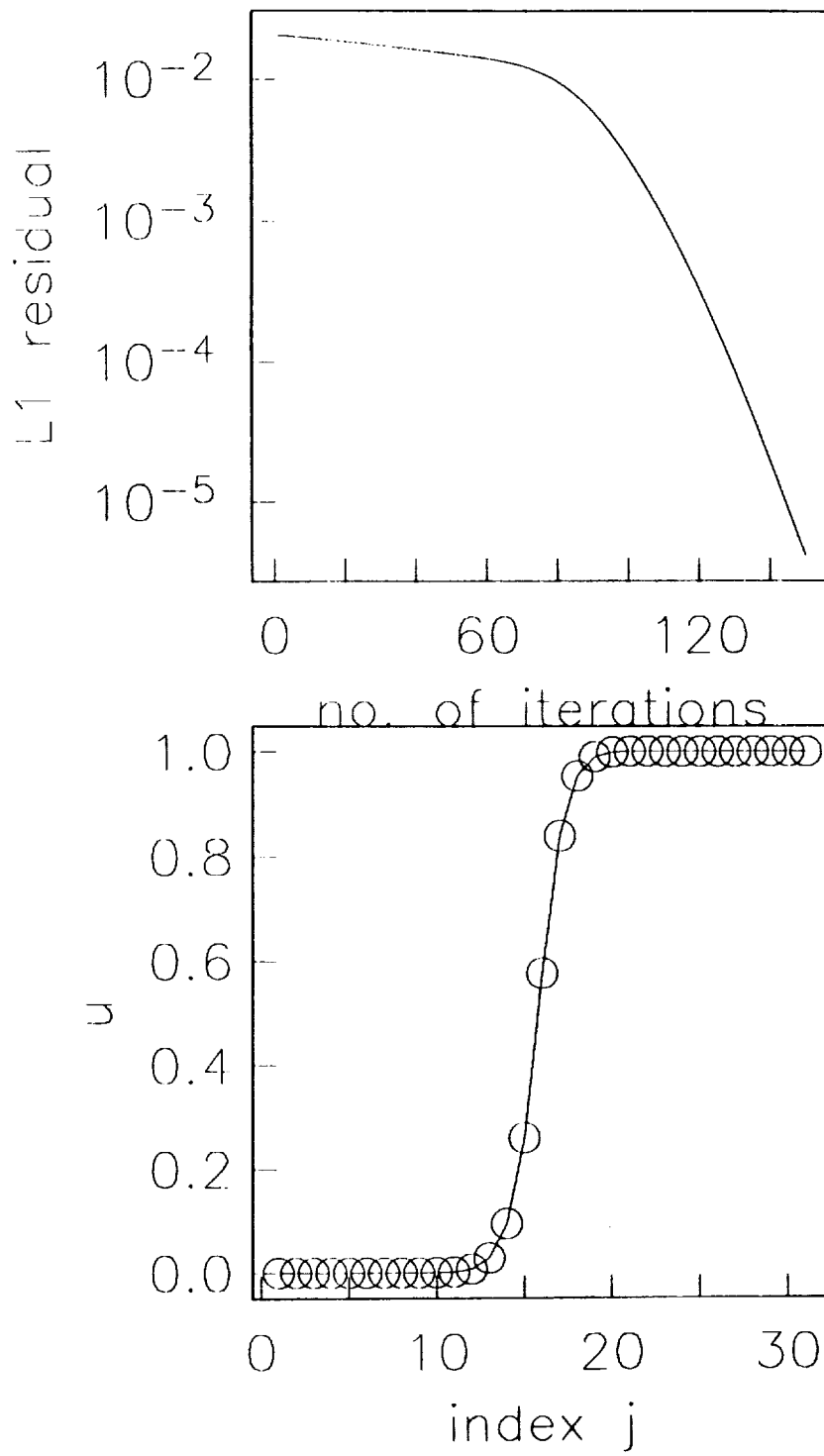Figure8(d) Problem 1, Scheme NN, isotropic mesh.

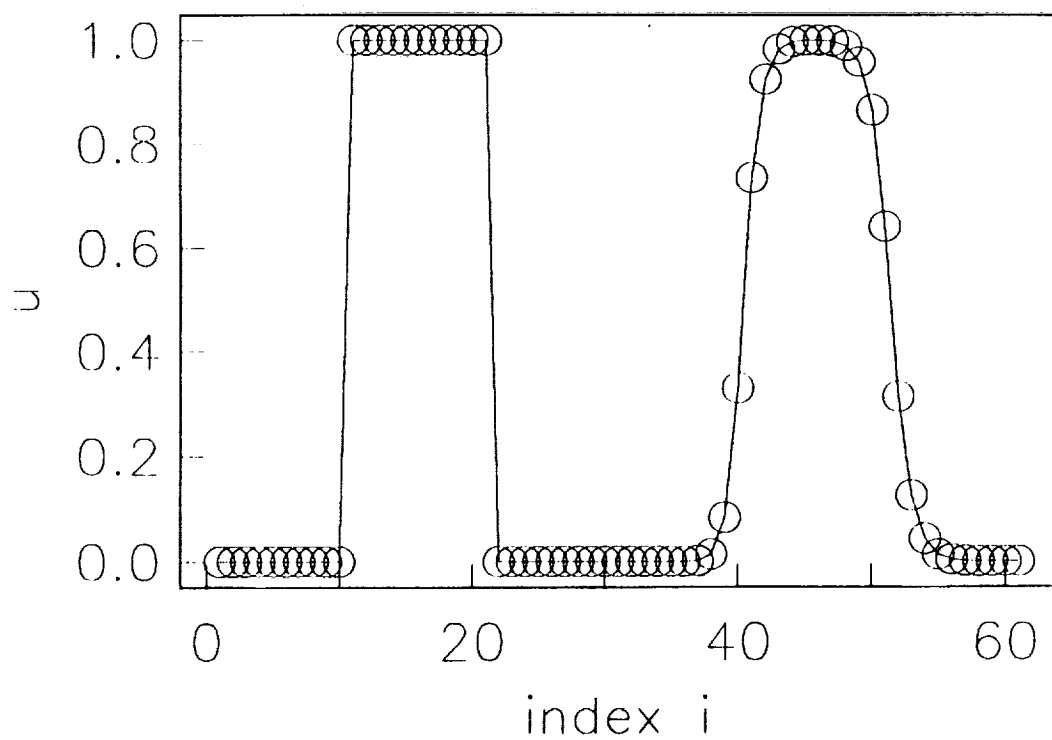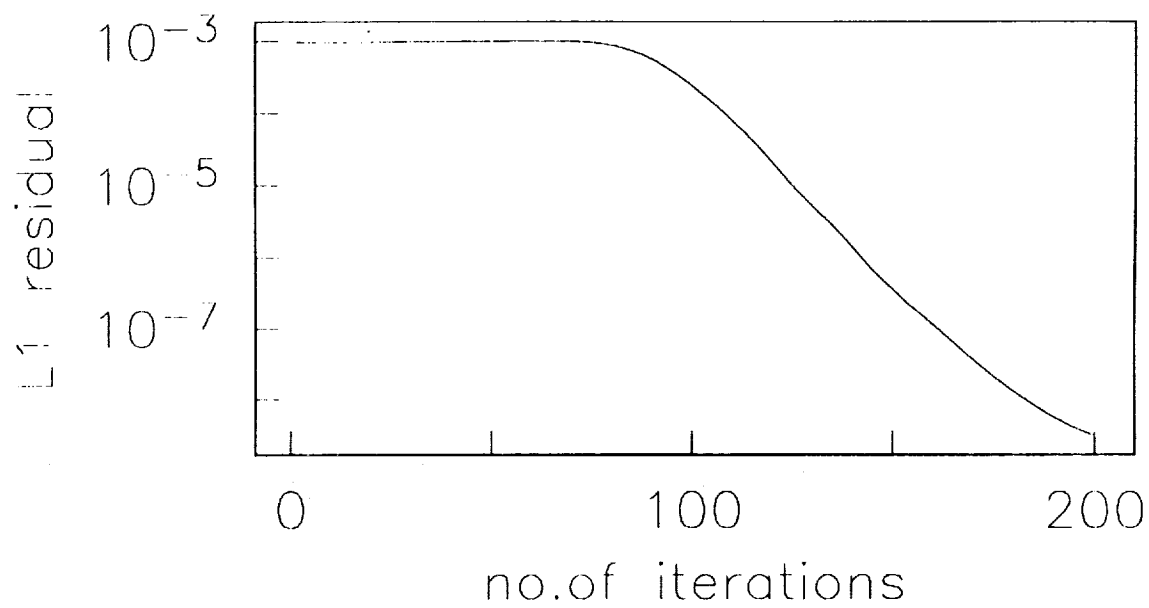Figure8(e) Problem 1, Scheme NN, correctly triangulated mesh.
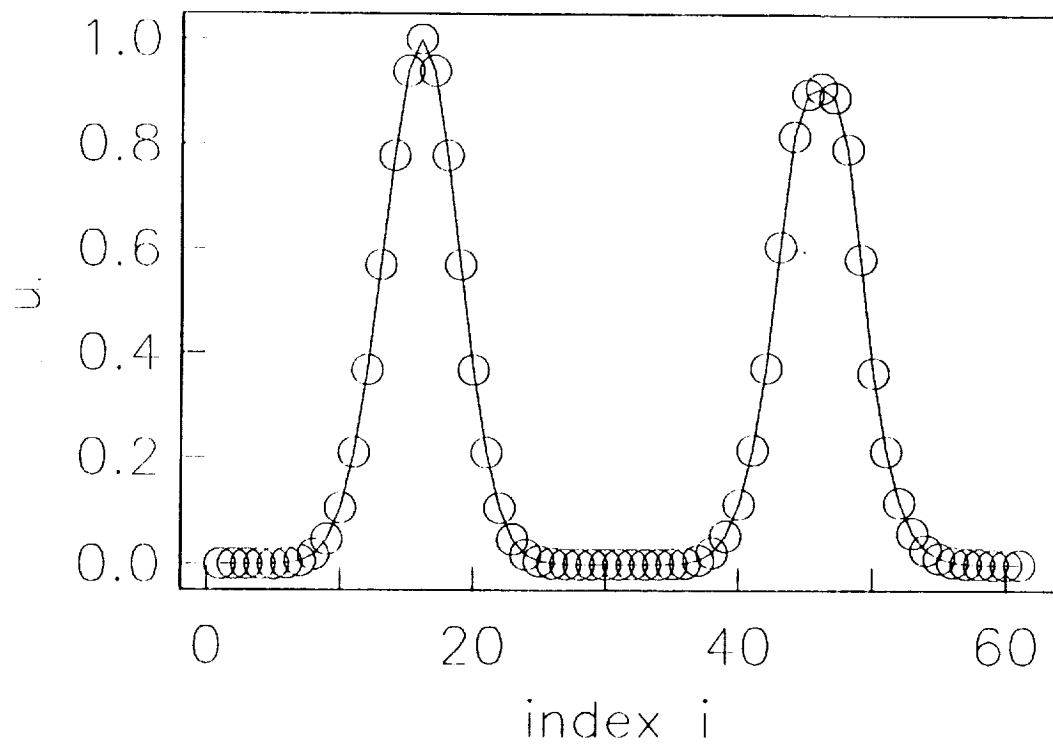
17
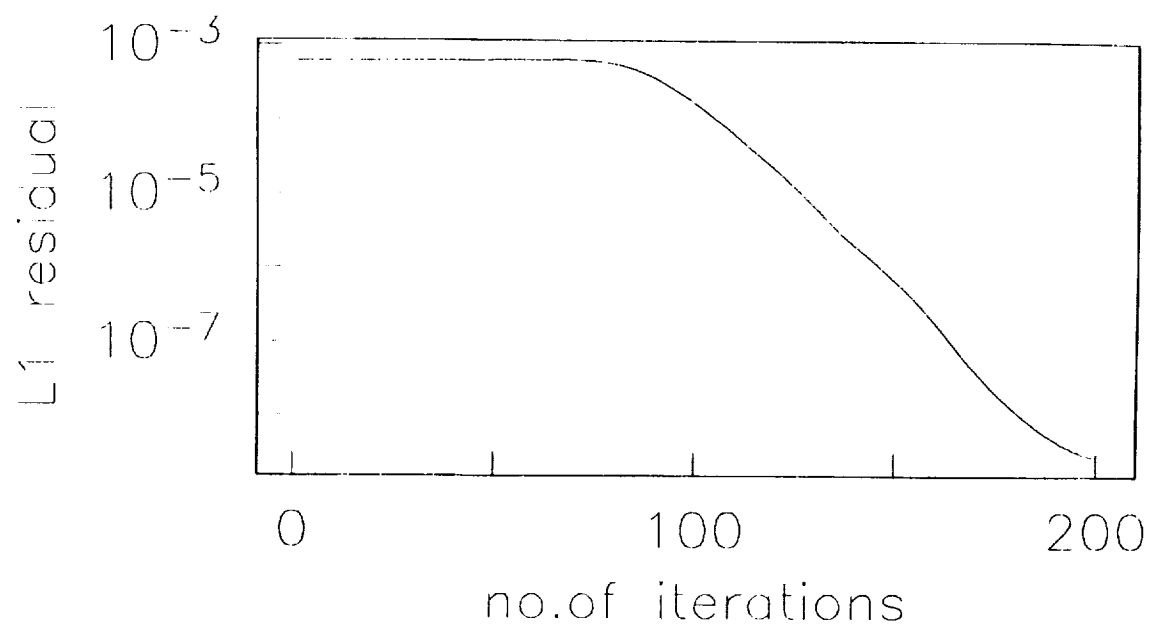
Figure9(a) Problem 2 – Scheme NN.

18

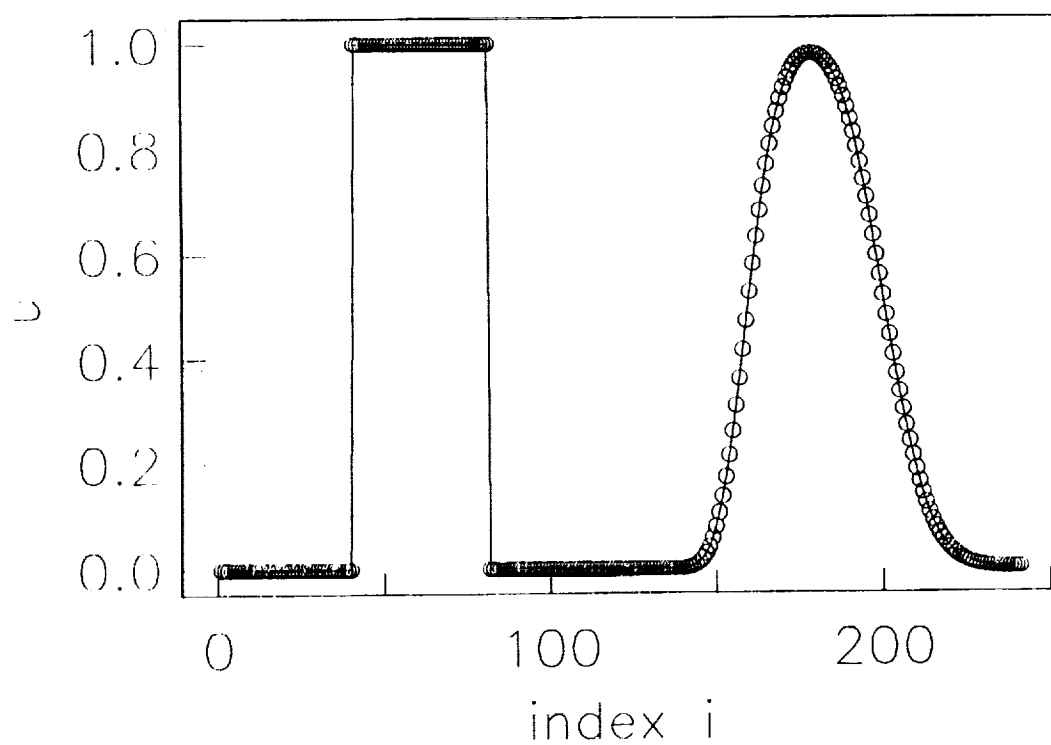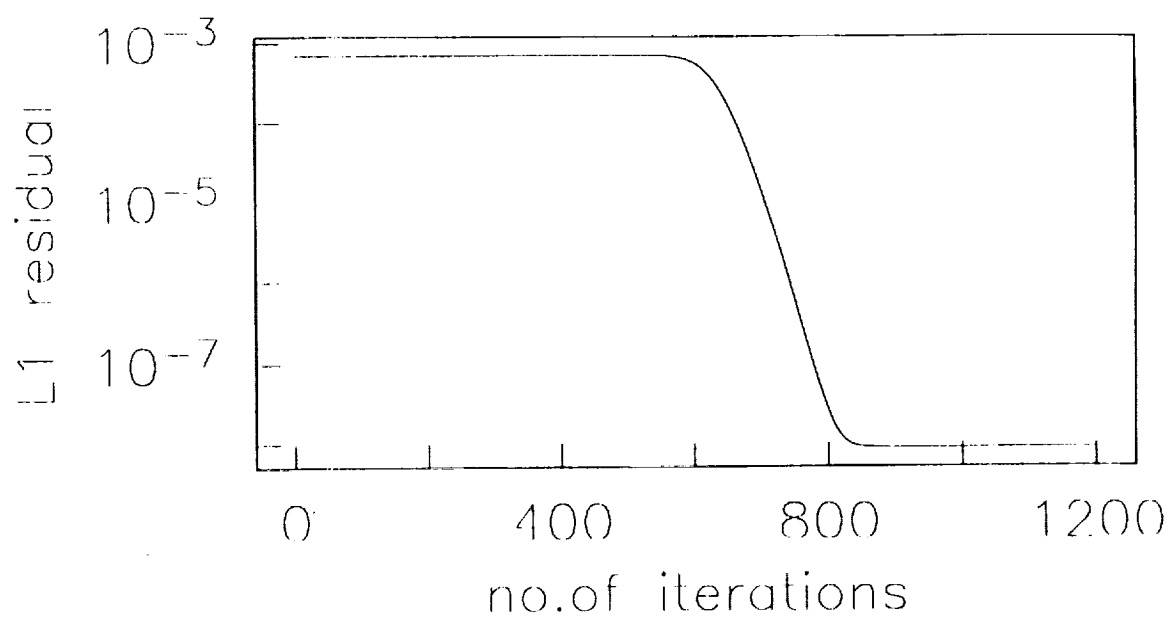Figure 9(b) Modified Problem 2 – Scheme NN.

Figure 9(c) Problem 2 – regular upwinding with mesh size 241 × 121.

Report Documentation Page

1. Report No. NASA CR-187459 ICASE Report No. 90-75	2. Government Accession No.	3. Recipient's Catalog No.
4. Title and Subtitle "OPTIMUM" UPWIND ADVECTION ON A TRIANGULAR MESH		5. Report Date October 1990
		6. Performing Organization Code
7. Author(s) P. L. Roe		8. Performing Organization Report No. 90-75
		10. Work Unit No. 505-90-21-01
9. Performing Organization Name and Address Institute for Computer Applications in Science and Engineering Mail Stop 132C, NASA Langley Research Center Hampton, VA 23665-5225		11. Contract or Grant No. NAS1-18605
		13. Type of Report and Period Covered Contractor Report
12. Sponsoring Agency Name and Address National Aeronautics and Space Administration Langley Research Center Hampton, VA 23665-5225		14. Sponsoring Agency Code

15. Supplementary Notes
Langley Technical Monitor: To be submitted to Journal Richard W. Barnwell   of Computational Physics Final Report

16. Abstract

For advection schemes based on fluctuation splitting, a design criterion on optimising the time step leads to linear schemes that coincide with those designed for least truncation error. A further stage of optimising the time step using a non-linear positivity criterion, leads to considerable further gains in resolution.

17. Key Words (Suggested by Author(s)) advection, multidimensional upwinding	18. Distribution Statement 34 - Fluid Mechanics and Heat Transfer 64 - Numerical Analysis Unclassified - Unlimited

19. Security Classif. (of this report) Unclassified	20. Security Classif. (of this page) Unclassified	21. No. of pages 22	22. Price A03